Application Note

Cell Analysis

Agilent

Trusted Answers

Three-Dimensional Multispheroid Assays Using the Agilent xCELLigence RTCA eSight

Powering cytotoxicity and immune cell killing assays

Authors

Tian Wang, Grace Yang, Yunfei Pu, Peifang Ye
Agilent Biosciences Co. Ltd., Hangzhou, China

Ryan Raver, Xiaoyu Zhang, Nancy Li
Agilent Technologies, Inc.

Abstract

With the emergence of three-dimensional (3D) scaffold-dependent cultures, researchers have gained the ability to partially mimic the tumor microenvironment, enabling more accurate testing of drug functionality and evaluation of chemoresistance within a 3D architecture that includes cell-cell and cell-extracellular matrix interactions. In this application note, we developed two scaffold-dependent multispheroid formation and monitoring assays. In method one, multispheroids were grown from cells on a Matrigel layer. In method two, multispheroids were grown from cells embedded in Matrigel. In both methods, the morphology, size, and viability of multispheroids changing over treatment and time were monitored using the brightfield and fluorescence imaging of the Agilent xCELLigence RTCA eSight system. Additionally, the Agilent xCELLigence RTCA eSight software includes advanced recognition and analysis functions that enable quantitative assessment of multispheroids. In conclusion, the 3D multispheroid assays developed using the xCELLigence RTCA eSight system provide a powerful and physiologically relevant platform for high-throughput immunotherapy and drug discovery studies.

Introduction

Cell-based assays are a key tool in basic research and drug discovery and are increasingly used in oncology research.[1] In recent years, a deeper understanding of how the tumor microenvironment influences drug response has driven a shift from traditional two-dimensional (2D) models to more advanced three-dimensional (3D) culture systems in antitumor therapeutic research. Unlike 2D models, where cells grow as a flat monolayer on artificial surfaces, 3D models allow cells to interact within a spatial structure that more closely resembles in vivo conditions. These models capture key features such as cellular heterogeneity, nutrient gradients, and hypoxic regions, making them essential for studying cancer progression and evaluating drug responses more accurately.[2]

Generally, 3D cell culture models are classified into two types: scaffold-free models, where cells naturally aggregate into a single spheroid at the bottom of an ultralow attachment (ULA) plate without the use of an extracellular matrix (ECM), and scaffold-dependent models, where cells are cultured within an ECM to support growth and structural organization.[3]

The 3D multispheroids model is one of the scaffold-dependent methods using a flat bottom plate on which the cells are deposited on an ECM layer or embedded in an ECM to generate multispheroids. Multispheroid tumors with ECMs have become an important tool in cancer research due to their ability to better replicate the complexity and heterogeneity of real tumors compared to single spheroid models. While single spheroids offer high reproducibility and resemble large solid tumors for drug testing, multispheroid models represent the diverse cellular makeup and microenvironmental interactions found in actual tumors more accurately.

As 3D spheroid techniques become more widely adopted, these models enable more advanced and translational studies. They also provide a rapid and effective platform for evaluating drug efficacy and toxicity in real time, making them highly valuable for preclinical oncology research. Despite these advancements, monitoring and analyzing multispheroids remains challenging, as traditional methods are often time-consuming, costly, and can disrupt the natural cell state. Additionally, commonly used surrogate markers—such as metabolic activity or cellular ATP—are often nonspecific and may miss valuable morphological insights.[4]

To address these challenges, we used the xCELLigence RTCA eSight system, which combines label-free techniques and nonperturbing reagents to enable noninvasive, real-time monitoring of multispheroid growth and shrinkage within physiologically relevant ECMs. This streamlined, high-throughput approach allows for precise analysis of cellular dynamics and treatment effects with minimal disruption. The integration of these technologies is expanding the potential for more accurate, reproducible cancer research and holds promise for improving the translational impact of preclinical studies.

Experimental

Cell maintenance and assays were conducted in an incubator at 37 °C/5% CO_2. The workflow is shown in Figure 1. Cell lines and their growth medium are shown in Table 1. Fetal bovine serum (FBS) was from Gibco (part number 10099-141), and penicillin/streptomycin (pen/strep)was from HyClone (part number SV30010).

Table 1. Cell lines utilized in 3D multispheroid studies with corresponding cell culture media conditions.

Cell Lines	Base Medium	Medium Supplements
A549	Ham's F-12K (Gibco, p/n 21127-022)	10% FBS (Gibco, p/n 10099-141) + 1% pen/strep (HyClone, p/n SV30010)
SKOV3	Moccy's 5A (Gibco, p/n 16600-082)	10% FBS (Gibco, p/n 10099-141) + 1% pen/strep (HyClone, p/n SV30010)
MCF7	DMEM (Gibco, p/n 12430-054)	10% FBS (Gibco, p/n 10099-141) + 1% pen/strep (HyClone, p/n SV30010)
BT474	Hybri-Care (ATCC, p/n 46-X)	10% FBS (Gibco, p/n 10099-141) + 1% pen/strep (HyClone, p/n SV30010)
PC3	Ham's F12 (Gibco, p/n 11765-054)	10% FBS (Gibco, p/n 10099-141) + 1% pen/strep (HyClone, p/n SV30010) + 1.5 g/L sodium bicarbonate

A549 Red cells, which express a nuclear-restricted red fluorescent protein, were produced by transducing the parental cells with the Agilent eLenti Red reagent (part number 8711011). Cells were shifted 72 hours after transduction to complete growth medium containing 2 µg/mL puromycin for an additional 14-day selection.

Before conducting multispheroid experiments, all culture plates, pipette tips, and reagents contacting the Matrigel (Corning, part number 254234) were prechilled. All Matrigel-related operations should be performed on ice. Table 2 lists the treatments used in this experiment.

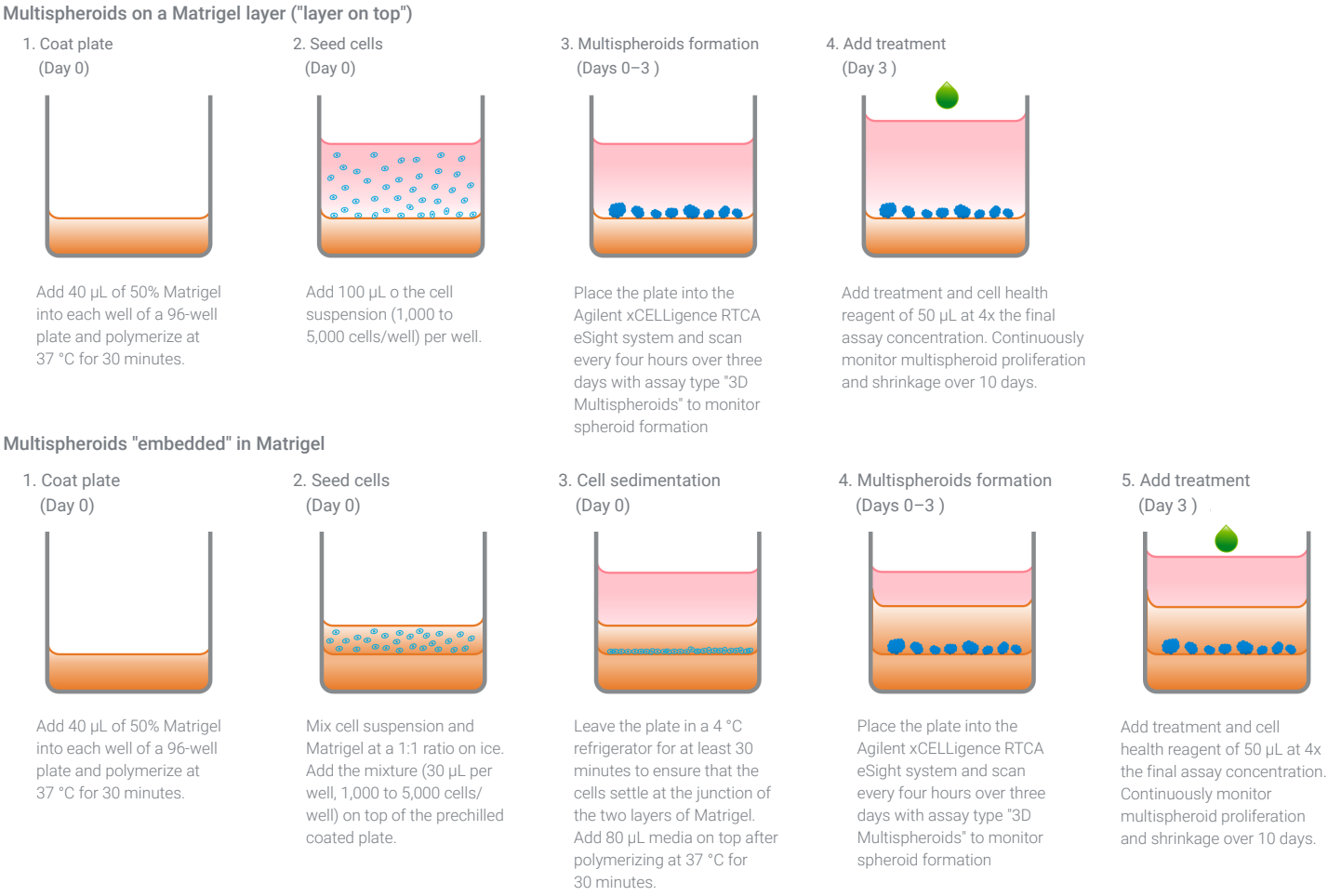

Figure 1. Workflow for the multispheroids assay.

Table 2. The treatments used in this experiment.

Treatments	Part Number	Dilution Factor	Concentration Range Supplements
Camptothecin	Sigma-Aldrich, p/n 390238	1:3	3 µM to 1.37 nM
Staurosporine	Sigma-Aldrich, p/n 569397	1:3	3 µM to1.37 nM
Taxol	Sigma-Aldrich, p/n 508227	1:2	300 to 2.34 nM
Trastuzumab Emtansine (T-DM1)	MedChemExpress, p/n HY-9921	1:2	3.2 to 25 ng/mL
Activated NK cells	OriBiotech, p/n FPB012-3	1:3	18,000 to 660 cells/well E:T 9:1 to 0.33:1

Procedure for the multispheroid assays

1. Coat each well of the 96-well flat-bottom plates with 40 µL of 50% Matrigel on day 0. Gently tap the plate edge to ensure that the Matrigel evenly covers the bottom of the well. Let the Matrigel polymerize at 37 °C for 30 minutes.
2. Seed cells.
   a. Multispheroids on a Matrigel layer: following trypsinization from the maintenance culture flask, the cells are centrifuged, resuspended, and counted. They are then seeded onto the solidified Matrigel at the appropriate density (110 µL/well). It is recommended to optimize the seeding density between 1,000 and 5,000 cells/well. **Note:** As a guide, we recommend seeding MCF7 at 1,000 to 2,000 cells/well; A549 at 2,000 to 3,000 cells/well; SKOV3, PC3, and BT474 at 2,000 to 4,000 cells/well.

b. Multispheroids embedded in Matrigel: mix the cell suspension and Matrigel at a volume ratio of 1:1 on ice gently. Add the mixture (30 µL/well, 1,000 to 5,000 cells/well) to the prechilled coated plate. Gently tap the edges of the culture plate to ensure an even distribution of cells and Matrigel. Then, leave the plate in a 4 °C refrigerator for at least 30 minutes to allow the cells to settle at the interface of the two layers of Matrigel, which is crucial for successfully focusing on the embedded multispheroids. Place the plate in a 37 °C incubator for 30 minutes to polymerize the Matrigel. After that, add 80 µL of complete medium to the top.

3. Place the 96-well flat-bottom plate on any of the five RTCA eSight cradles (v1.4.0 software or later required and balance for 15 minutes before starting the acquisition.
4. Monitor spheroid formation for 72 hours and schedule the image acquisition as: 10x objective 2 x 2 stitch or 5x objective one image/well. Set the exposure time of the red and green channels to 50 to 200 ms (depending on the fluorescent brightness) and acquire images every four hours.
5. On day three, add small molecular drugs, antibody-drug conjugate (ADC), or immune cells separately (Table 2), or simultaneously with Agilent eTox green reagent (part number 8711008) at a 4x final assay concentration (50 µL/well) after the multispheroid formation. Multiplexing is also possible using Agilent eCaspase reagent (part number 8711005) and Agilent eAnnexin reagents (part numbers, 8711006, 8711007, 8711026) to specifically monitor apoptosis.
6. Continuously monitor the growth and shrinkage of the multispheroids using the xCELLigence RTCA eSight system (four-hour scan interval, up to two weeks). Quantify the response of multispheroids based on label-free brightfield images and fluorescence images.

Results and discussion

Generation of multispheroids from various cell lines

MCF7, A549, SKOV3, PC3, and BT474 cells were seeded at 3,000 cells/well and allowed to form multispheroids. Different cell lines showed distinctive morphologies. A549, BT474, and MCF-7 cells formed smooth, round spheroids, while SKOV3 and PC3 spheroids showed varying degrees of stellate branching, indicative of invasion morphology (Figure 2). The yellow outline mask demonstrates that xCELLigence RTCA eSight software delivers robust and precise recognition of spheroids with diverse morphologies, establishing a strong foundation for its role as a powerful tool in downstream analysis.

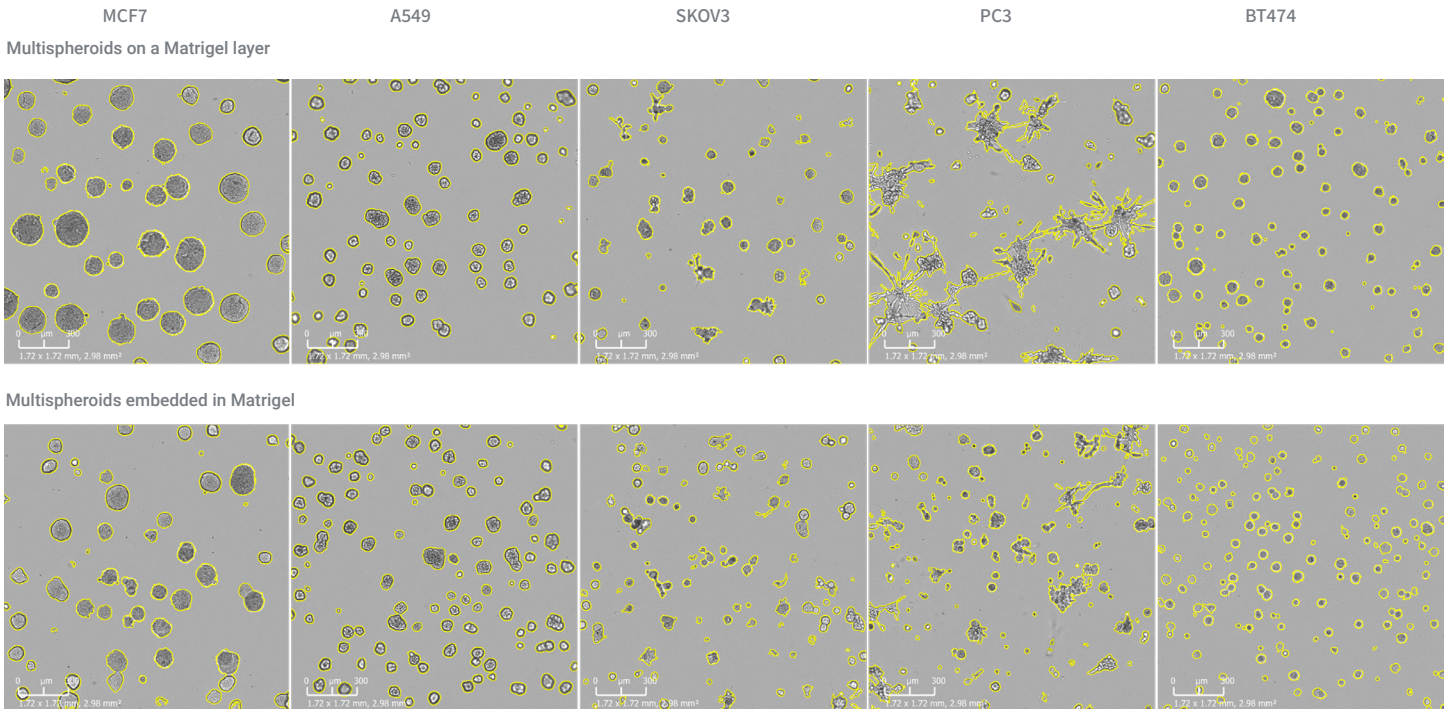

Figure 2. Brightfield images of multispheroids formed from a range of tumor cell lines on a Matrigel layer (top) or embedded in Matrigel (bottom). Representative images were taken seven days after cell seeding using a 10x objective.

Cell seeding density optimization

To determine the optimal seeding density, serial dilutions of A549 cells, from 1,000 cells/well up to 5,000 cells/well, were seeded on the Matrigel layer. The images and the quantitative growth curves show that both the total spheroid area (as indicated by brightfield total area) and the individual spheroid size (as indicated by brightfield average area) increased with increasing seeding density (Figure 3). When determining the optimal seeding density, several factors were considered. The first was the individual spheroid size, with a uniform spheroid diameter close to or larger than 100 µm at the treatment time (72 hours postseeding),[3] necessitating a higher cell seeding density ≥ 1,000 cells/well (Figure 3D).The second factor was the growth of the spheroids, keeping growth in a long term to reflect the treatment effect on spheroid growth, where Figure 3B suggested that seeding density ≤ 3,000 cells/well, spheroids kept growing for up to six days, while 4,000 and 5,000 densities plateaued around 120 hours. The third factor was maintaining a steady spheroid count to avoid frequent fusion, where spheroid fusion is evidenced by decreased brightfield object counts at 4,000 and 5,000 densities over times (Figure 3C). Based on these factors, 2,000 to 3,000 cells/well is an appropriate seeding density for A549 cells.

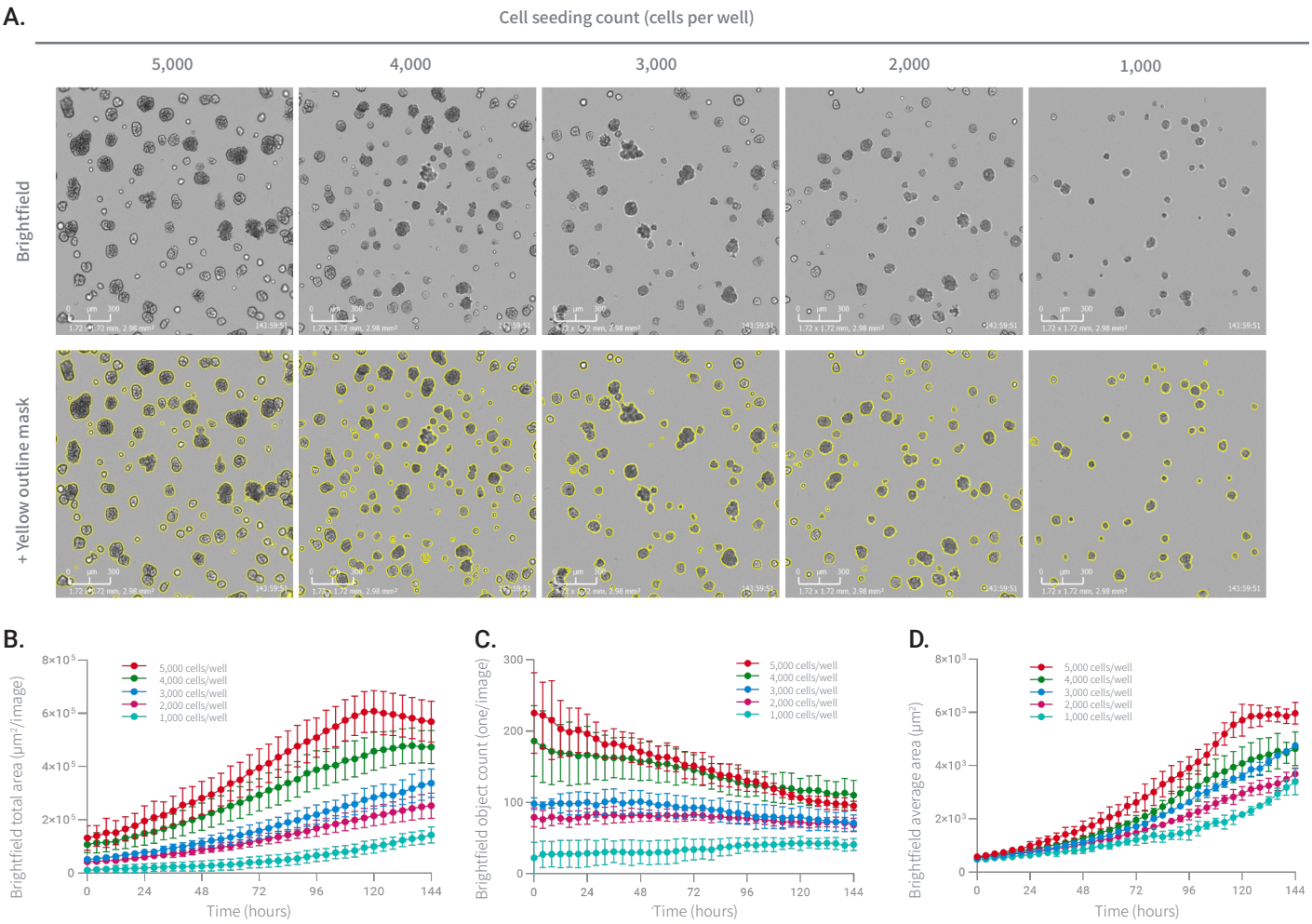

Figure 3. Titration of cell seeding density. A549 cells were seeded on a Matrigel layer at various densities (1,000 to 5,000 cells/well). (A) Typical brightfield images and spheroid recognition based on brightfield 168 hours after cell seeding. (B) The brightfield total area over time plot. (C) The brightfield object count over time plot. (D) The brightfield average area over time plot.

Cytotoxicity of multispheroids formed from various cell lines

The multispheroid assay conducted on the xCELLigence RTCA eSight enables label-free drug cytotoxicity evaluation. Here, the size changes of MCF7, SKOV3, and PC3 multispheroids on the Matrigel layer (Figure 4A) or embedded in the Matrigel (Figure 4B) reflect the cytotoxicity of the small molecular DNA topoisomerase I inhibitor camptothecin and vehicle control (0.1% DMSO). Time course brightfield total area curves reveal that the sizes of multispheroids in the control group increased significantly over 168 hours, while multispheroids treated with camptothecin either decreased or did not change over time. In short, camptothecin inhibits the proliferation of multispheroids derived from all tested cell lines.

Dose-dependent cytotoxicity of A549 multispheroids

The xCELLigence RTCA eSight system has the capability of fluorescence imaging and analysis alongside label-free brightfield analysis in both multispheroid assays developed in this application note. Stable expression of a nuclear-restricted fluorescent protein in multispheroids provides insights into cell viability, where growth increases fluorescence, and cytotoxicity reduces fluorescence. Over seven days, A549 red multispheroids treated with various camptothecin doses showed a concentration-dependent reduction in brightfield and red fluorescence areas (Figure 5). In addition, eTox green selectively stains the nuclei of dead cells, which enables real-time monitoring of cell death in response to camptothecin treatment (Figure 5A). The IC50s calculated by the RTCA

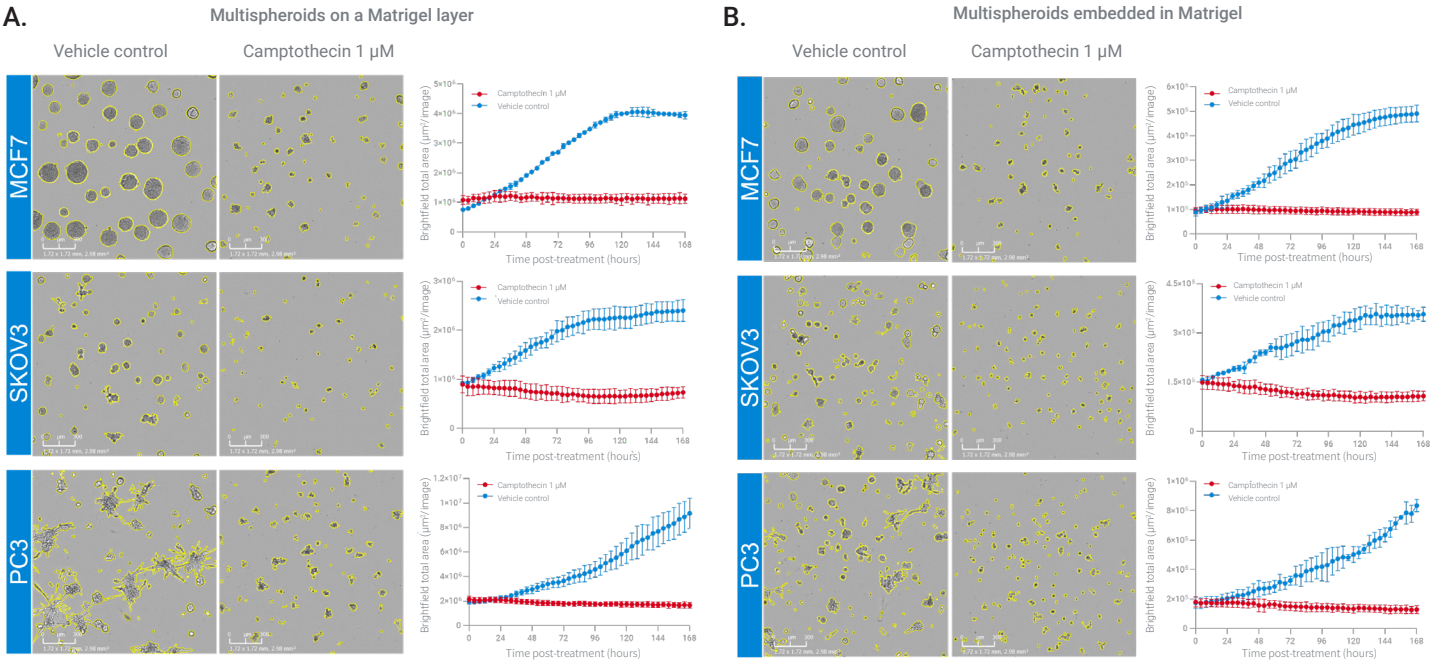

Figure 4. The cytotoxicity of camptothecin on multispheroids derived from different cell lines, MCF-7, SKOV3, and PC3. Cells were seeded in flat-bottom 96-well plates (3,000 cells/well) on a Matrigel layer or embedded in Matrigel. Spheroids were allowed to form for 72 hours and then treated with either vehicle (0.1% DMSO) or camptothecin (1 µM) for 168 hours. Images were captured using 10x magnification at four-hour intervals. The images were acquired 168 hours posttreatment. (A) Multispheroids on a Matrigel layer. (B) Multispheroids embedded in Matrigel. Yellow lines are spheroid recognition mask outlines based on brightfield images. Time course plots show the brightfield total area over 168 hours posttreatment (mean ± SD, n = 4).

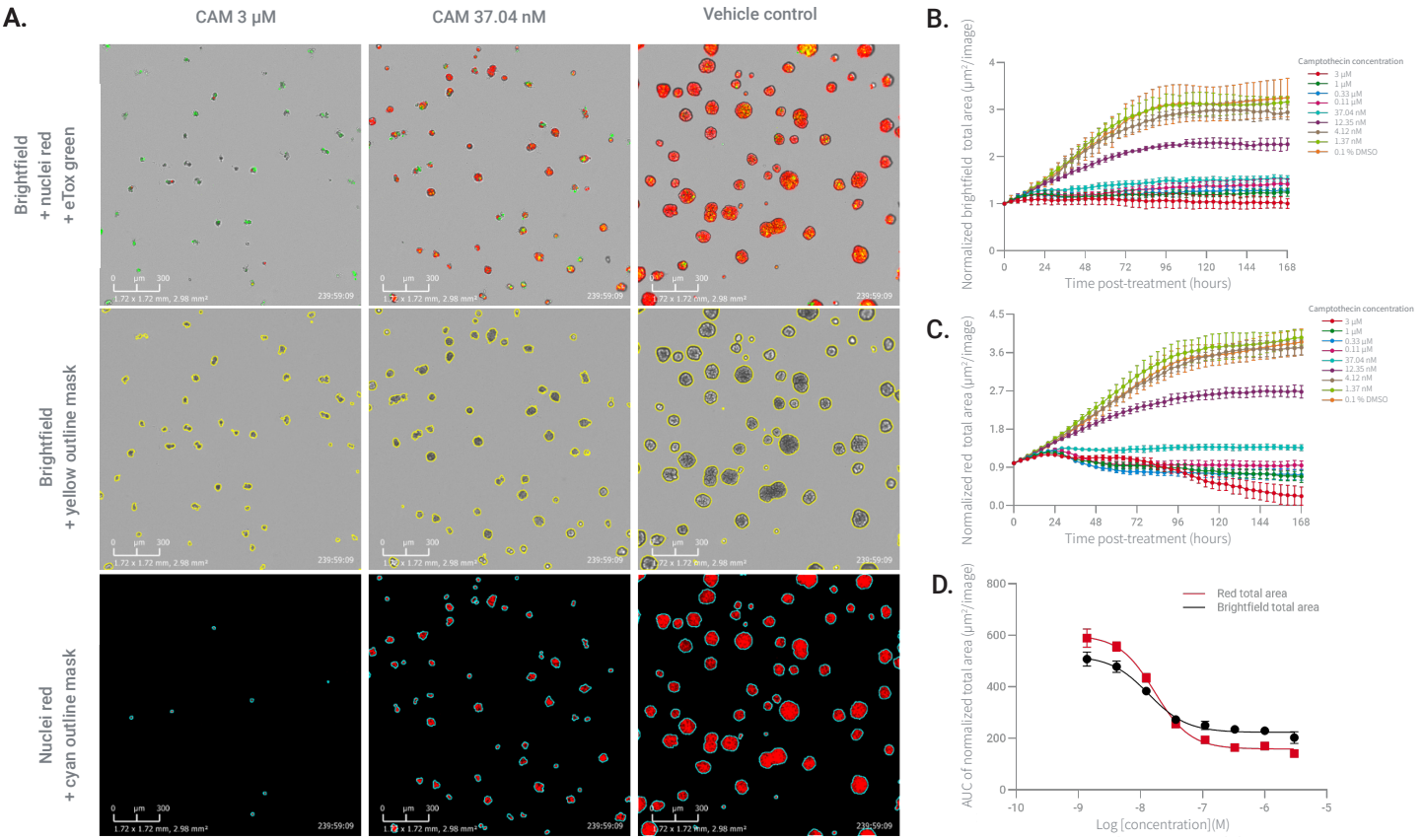

Figure 5. Quantification of cytotoxicity on multispheroids using brightfield and fluorescent readouts. A549 red cells (2,000 cells/well) were seeded on a Matrigel layer and formed multispheroids for three days. Then multispheroids were treated with camptothecin gradients (3 µM to 1.37 nM) or vehicle control (0.1% DMSO) in the presence of eTox green (250 nM). Images of brightfield, red, and green channels were captured every four hours for up to 10 days with 10x magnification. (A) Representative images taken seven days after treatment show camptothecin concentration-dependent inhibition of A549 spheroids growth, present as brightfield and red total area decreasing (B and C) when camptothecin concentration increases. (D) The IC50, calculated by Agilent xCELLigence RTCA eSight software using the area under the curve (AUC) of normalized brightfield and red total area from 0 to 7 days after treatment (mean ± SD, n = 3).

eSight software using the area under the curve of normalized brightfield or red total area were 13.5 and 17.0 nM (Figure 5D), respectively. Notably, 3 µM camptothecin treatment over seven days resulted in a near-total loss of red fluorescence while brightfield cell fragments were still detectable (Figures 5B and C). To demonstrate the application of these 3D multispheroid models in drug toxicity tests, a high-throughput pharmacological study was conducted using a panel of small-molecule toxic drugs: camptothecin, protein kinase inhibitor staurosporine, and natural antitumor agent taxol. Each compound produced a concentration-dependent inhibition of spheroid growth, with the area under the curve (AUC) analysis showing close IC50 values from multispheroids cultured on a Matrigel layer and multispheroids embedded in Matrigel (Figure 6). This reflects that the infiltration of small-molecule drugs is almost not influenced by the surrounding Matrigel.

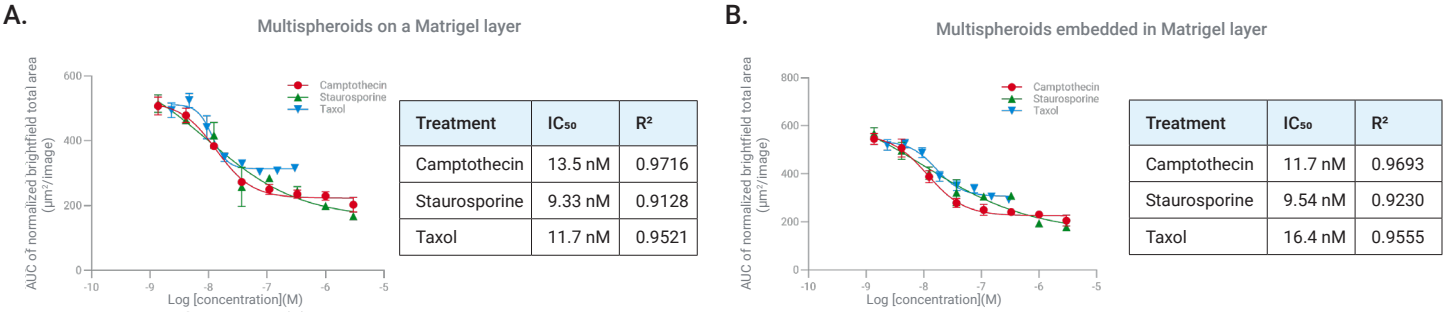

Treatment	IC_{50}	R^2
Camptothecin	13.5 nM	0.9716
Staurosporine	9.33 nM	0.9128
Taxol	11.7 nM	0.9521

Treatment	IC_{50}	R^2
Camptothecin	11.7 nM	0.9693
Staurosporine	9.54 nM	0.9230
Taxol	16.4 nM	0.9555

Figure 6. Effect of camptothecin, staurosporine, and taxol on A549 multispheroids. A549 cells were plated at a density of 2,000 cells/well, and multispheroids were allowed to form (for three days) on a (A) Matrigel layer or (B) embedded in Matrigel. Multispheroids were then treated with serial dilutions of compounds (camptothecin: 3 μM to 1.37 nM; staurosporine: 3 μM to 1.37 nM; taxol: 300 to 2.34 nM), and the kinetics of spheroid growth were obtained. Concentration-response curves represent the area under the curve of the normalized brightfield total area time course from 0 to 7 days after treatment. (mean ± SD, n = 4 wells).

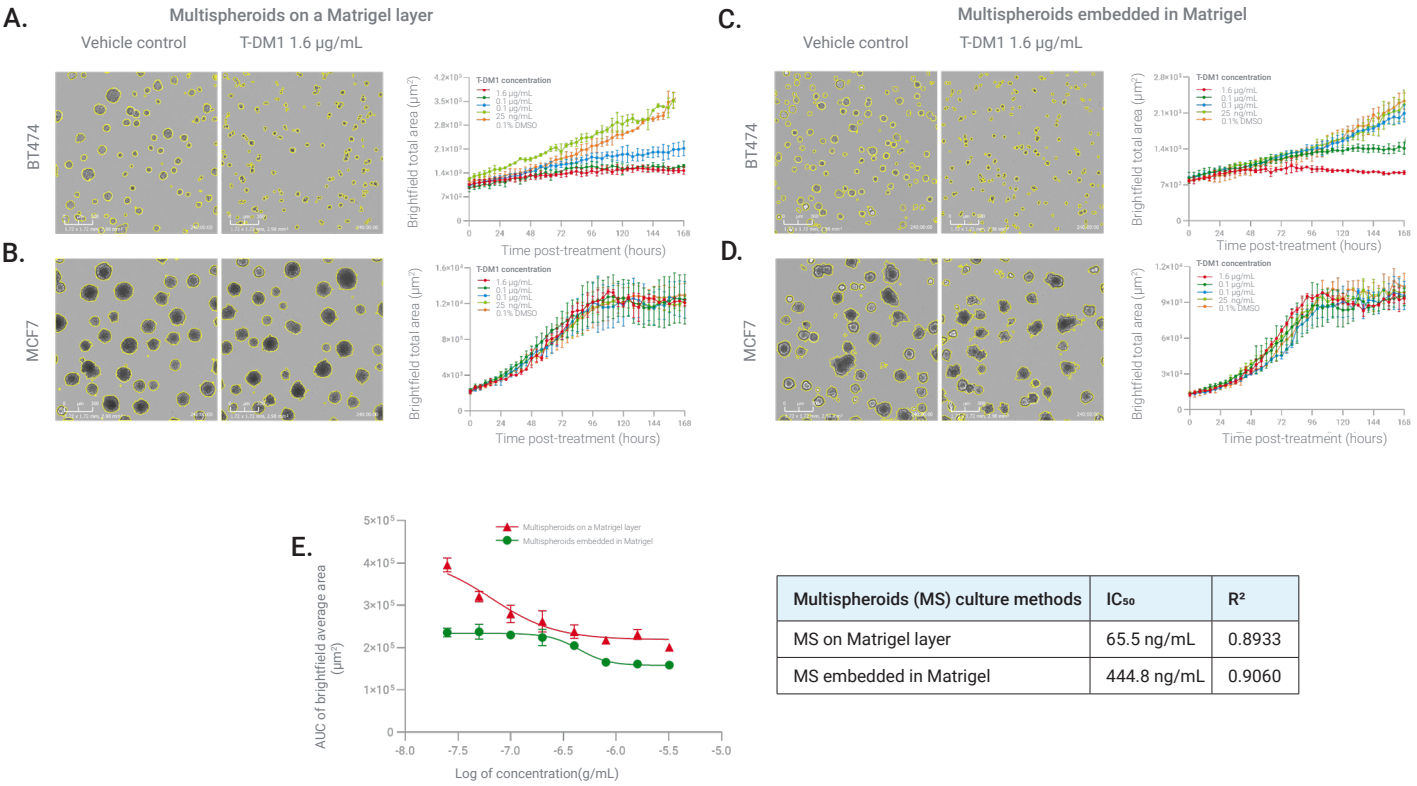

Multispheroids (MS) culture methods	IC_{50}	R^2
MS on Matrigel layer	65.5 ng/mL	0.8933
MS embedded in Matrigel	444.8 ng/mL	0.9060

Figure 7. Effects of HER2 targeting T-DM1 on multispheroids formed by (A and C) HER2-positive BT474 or (B and D) HER2-negative MCF7. BT474 and MCF7 cells were seeded at a density of 4,000 and 2,000 cells/well, respectively. Multispheroids were allowed to form (for three days) on a Matrigel layer or embedded in Matrigel, and then treated with varying concentrations of T-DM1. Representative images of multispheroids on Matrigel layer (A and B) and multispheroids embedded in Matrigel (C and D) with yellow mask outlines at 168 h (seven days after treatment) were shown. Normalized brightfield total area of (A and C) BT474 and (B and D) MCF7 multispheroids were plotted as a function of time. (E) Dose-response-curves generated from A and C (mean ± SD, n = 4).

ADC drug induced cytotoxicity on multispheroids

In addition to the small molecular drugs, we also evaluated the feasibility of the multispheroid model for assessing the specificity and potency of ADCs. T-DM1 is a trastuzumab-DM1 conjugated drug targeting HER2-positive cancer cells. The multispheroids formed by HER2-positive BT474 cells or HER2-negative MCF7 cells were used to assess the cytotoxicity and specificity of T-DM1. In Figure 7, both images and quantitative analysis curves show that T-DM1 induced a concentration-dependent slowing growth of BT474 spheroids (Figure 7A and C) but did not influence the growth of MCF7 spheroids (Figure 7B and D). Comparing Figures 7A and 7C, 0.1 µg/mL T-DM1 treatment significantly inhibited the growth of multispheroids on Matrigel but had little effect on embedded multispheroids. The IC50 values calculated from curves in Figure 7A and 7C are 65.5 and 444.8 ng/mL, respectively (Figure 7D). In conclusion, compared to the semi-open environment on a Matrigel layer, the fully surrounding Matrigel appears to impede the penetration of macromolecular ADC drugs, leading to increased resistance in the embedded multispheroids.

NK cells killing of multispheroids

Fluorescent labeling is an effective strategy to distinguish effector cells from target cells in a coculture situation. In this assay, in vitro activated human NK cells were cocultured with multispheroids formed by A549 cells expressing red fluorescent proteins in the nucleus. NK cell killing of multispheroids was monitored in real-time and quantified with the fluorescence intensity of A549 cells.

From Figure 8, NK cells induced an E:T ratio-dependent killing of A549 red multispheroids (Figure 8A) as the red total area decreases over time in both multispheroid models as the E: T ratio increases (Figure 8B and C). Since NK cells need to invade through the Matrigel that sits on top of the multispheroids, the killing of multispheroids embedded in Matrigel was delayed and less strong. At an E:T ratio of 9:1, NK cells achieved ~ 30% cytolysis of multispheroids embedded in Matrigel compared to ~ 50% cytolysis for those layered on top of a Matrigel layer (Figure 8D).

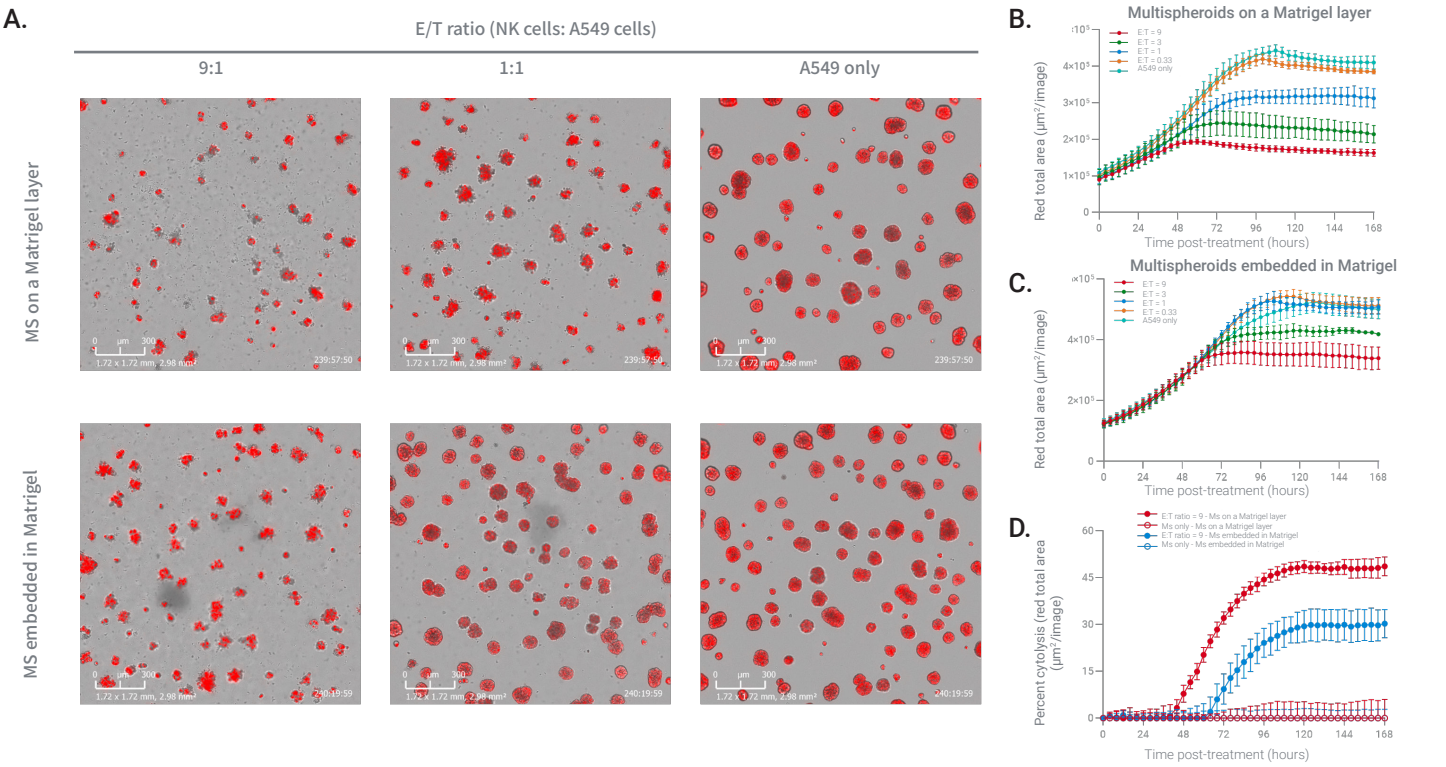

Figure 8. Natural killer (NK) cells killing of multispheroids in an E:T ratio dependent manner. A549 red cells were seeded at a density of 2,000 cells/well, and multispheroids were allowed to form (for 72 hours) on the Matrigel layer or embedded in Matrigel. NK cells were added to multispheroids at varying E:T ratios and changes were monitored. (A) Representative images at 168 hours after treatment. Red total area of (B) multispheroids on a Matrigel layer or (C) multispheroids embedded in Matrigel as a function of time. (D) Comparison of the NK cell killing efficacy on multispheroids on a Matrigel layer or those embedded in Matrigel by percent cytolysis (red total area) with E:T = 9. Percent cytolysis (red total area) was calculated and plotted as a function of time (0 to 7 days after treatment) using the immunotherapy module (part number S2807-90051) of Agilent xCELLigence RTCA eSight software.
Percent cytolysis = (1 - (normalized red total area of sample wells) / (average normalized red total area of reference wells)) × 100 (mean ± SD, n = 4).

Conclusion

In this study, we developed two 3D multispheroid culture methods with spheroids either formed on a Matrigel layer or embedded within Matrigel. We demonstrate that the Agilent xCELLigence RTCA eSight system, combined with the 3D multispheroids module and Agilent lentivirus reagents, enables convenient, label-free brightfield and fluorescence analysis to monitor spheroid morphology, viability, and shrinkage over time. Our results confirmed successful generation and growth of 3D multispheroids using both methods. In cytotoxicity assays, both approaches showed comparable potency for small-molecule drugs, while spheroids embedded in Matrigel exhibited greater resistance to ADC drugs compared to those on a Matrigel layer, suggesting reduced drug penetration in the embedded model. Similarly, in immune cell killing assays, NK cell-mediated destruction of spheroids embedded in Matrigel was delayed and less effective than on the Matrigel layer, indicating more limited NK cell infiltration in the embedded spheroids. Users can select the most suitable method based on their specific research goals and the characteristics of their samples.

In conclusion, the 3D multispheroid assays established here, using the Agilent xCELLigence RTCA eSight system, provide a powerful and physiologically relevant platform for high-throughput drug toxicity assessment, discovery and development.

References

1. Horvath, P.; Aulner, N.; Bickle, M.; Davies, A. M.; Del Nery, E.; Ebner, D.; Montoya, M. C.; Östling, P.; Pietiäinen, V.; et al. Screening out irrelevant cell-based models of disease. *Nat. Rev. Drug Discovery*. **2016**,*15* (11), 751-769. DOI:10.1038/nrd.2016.175
2. Verjans, E.T.; Doijen, J.; Luyten, W.; Landuyt, B.; Schoofs, L. Three-dimensional cell culture models for anticancer drug screening: Worth the effort?. *J. Cell. Physiol*. **2018**, *233* (4), 2993-3003. DOI:10.1002/jcp.26052
3. Lee, S.Y.; Teng, Y.; Son, M.; Ku, B.; Moon, H. S.; Tergaonkar, V.; Chow, P. H.-H.; Lee, D. W.; Nam, D. H. High-dose drug heat map analysis for drug safety and efficacy in multi-spheroid brain normal cells and GBM patient-derived cells [correction *PLoS One*. **2023,** *18* (12). DOI: 10.1371/journal.pone.0295827]. *PLoS One*. **2021**, *16* (12). DOI:10.1371/journal.pone.0251998
4. Jabs, J.; Zickgraf, F.M.; Park, J. Wagner, S.; Jiang, X.; Jechow, K.; Kleinheinz, K.; Toprak, U. H.; Schneider, M. A.; Meister, M.; et al. Screening drug effects in patient-derived cancer cells links organoid responses to genome alterations. *Mol. Syst. Biol*. **2017**,*13* (11),955. DOI:10.15252/msb.20177697

Products used in this application

Agilent products

Agilent xCELLigence RTCA eSight

www.agilent.com

RA260114.592

Published in the USA, February 24, 2026
5994-8566EN

Agilent
Trusted Answers